AIP | Applied Physics Letters

Fermi-level band filling and band-gap renormalization in Ga-doped ZnO

J. D. Ye, S. L. Gu, S. M. Zhu, S. M. Liu, Y. D. Zheng et al.

Citation: Appl. Phys. Lett. **86**, 192111 (2005); doi: 10.1063/1.1928322
View online: http://dx.doi.org/10.1063/1.1928322
View Table of Contents: http://apl.aip.org/resource/1/APPLAB/v86/i19
Published by the American Institute of Physics.

Fermi-level band filling and band-gap renormalization in Ga-doped ZnO

J. D. Ye, S. L. Gu,[a] S. M. Zhu, S. M. Liu, Y. D. Zheng, R. Zhang, and Y. Shi
Department of Physics, Nanjing University, Nanjing 210093, People's Republic of China

(Received 20 December 2004; accepted 30 March 2005; published online 6 May 2005)

The fundamental optical properties of Ga-doped ZnO films grown by metalorganic chemical vapor deposition were investigated by room-temperature transmittance and photoluminescence (PL) spectroscopy. The Burstein–Moss (BM) shift of the absorption edge energy is observed at the carrier concentration up to 2.47×10^{19} cm^{-3}. The absorption edges are fitted to a comprehensive model based on the electronic energy-band structure near critical points plus relevant discrete and continuum excitonic effects, taking account of the Fermi-level filling factor. The theoretical calculation for BM effect is in good agreement with the experimental facts, considering the nonparabolic nature of conduction-band and band-gap renormalization (BGR) effects. Meanwhile, the monotonic redshift of the near-band-gap emission detected by PL measurements has also been observed with increasing free-carrier concentration, which is attributed to the BGR effects, and can be fitted by an $n^{1/3}$ power law with a BGR coefficient of 1.3×10^{-5} meV cm. © *2005 American Institute of Physics*. [DOI: 10.1063/1.1928322]

In spite of impressive achievements in epitaxial growth and device fabrication on ZnO,[1–4] many fundamental optical properties of impurity-doped ZnO films, particularly the Fermi-level band filling and band-gap renormalization (BGR) effects, which are of crucial importance in fabricating devices, are still in need of detailed description. Many research groups have evaluated the Burstein–Moss (BM) and BGR effects in Si-doped GaN and AlGaN materials.[5–7] Reynolds *et al.*[8] found that the energy of optical transitions in undoped ZnO and GaN films is the result of blueshift due to free-carrier screening and the redshift due to renormalization. However, due to the lack of heavily doped ZnO crystal in high crystallinity, less attention has so far been paid to the systematic and detailed investigation of BM and BGR effects in impurity-doped ZnO films. Recently, Makino *et al.*[9] demonstrated the radiative efficiency, threshold energy, and linewidth of the near-band-edge (NBE) transition energy in ZnO: Ga epilayers as a function of doping density of Ga. The effects of intentional doping and potential fluctuation on optical properties have not been fully studied yet. In this letter, we present a detailed study of the BM and BGR effects on the NBE transition in the metalorganic chemical vapor deposition (MOCVD) growth of Ga-doped ZnO single-crystal epilayers, including the comprehensive comparisons of experimental facts with the theoretical simulations.

The ZnO: Ga samples (S0-S3) were grown by low-pressure MOCVD technique on *c*-plane 2 in. sapphire substrates with low-temperature ZnO nucleation layers. Diethylzinc, 5N-purity O_2, and triisopropylgallium were used as Zn, O, and Ga sources, respectively. The growth temperature was 450 °C and the thickness of ZnO: Ga epilayers are approximately 300 nm. In our study, no obvious variation of thickness was observed for different dopant concentrations. The Ga concentration is varied from 0.0 at. % to 6.3 at. %, determined by adjusting the temperature of TIPGa MO source. Carrier concentrations were evaluated by capacitance-voltage (*C-V*) method using a mercury probe as Schottky contact. The measured values are summarized in Table I. Free-carrier concentration is monotonically modulated from 3.30×10^{15} up to 2.47×10^{19} cm^{-3} as the doping concentration increased except for the highest doping level. As for the sample grown with high Ga concentration up to 6.3 at. %, the carrier concentration decreased greatly, which is due to the presence of lattice defect complexes, such as (Ga_{Zn}–O_i) and (Ga_{Zn}–V_{Zn}), created by the excessive incorporation of Ga atoms into ZnO.[10,11] Photoluminescence (PL) measurements were carried out at room temperature, excited by a He–Cd laser (325 nm) with the incident power density of 40 mW/cm^2. Transmittance spectra were recorded using an UV/Visible spectrometer (U-3410, Hitachi).

Figure 1 shows typical room-temperature PL spectra of Ga-doped ZnO epilayers with Ga dopant concentration of 6.3 at. %. The spectra were dominated by the NBE optical transition around 3.29 eV in company with the weak deep level emission, indicative of high radiative efficiency and excellent optical properties in spite of highly Ga doping. The inset of Fig. 1 shows the NBE transition of samples with different Ga dopant concentration. Assuming the peak position of the NBE transition to be a measure of band-gap energy (E_{PL}), E_{PL} of samples is shifted from 3.298 eV to 3.260 eV as the dopant concentration increases from 0.0 at. % to 3.2 at. %. However, at a high Ga concentration of 6.3 at. %, E_{PL} of sample S3 increased again to 3.288 eV due to the decreased free-carrier concentration of 5.01×10^{17} cm^{-3}. We find that E_{PL} shows a monotonic redshift with increasing carrier concentration rather than the dopant concentration. Thus, it is

TABLE I. Samples specification for the four *n*-ZnO samples: Carrier concentrations of *n* are obtained by the *C-V* method; the absorption (Fermi-level) energy of E_{abs}, effective temperature of kT^* are deduced from Eq. (2).

Sample	R_{Ga} (%)	n(cm^{-3})	E_{abs} (eV)	kT^* (meV)
S0	0.0	3.30×10^{15}	3.301	95
S1	0.9	1.15×10^{17}	3.309	107
S2	3.2	2.47×10^{19}	3.387	113
S3	6.3	5.01×10^{17}	3.307	109

[a]Author to whom correspondence should be addressed; electronic mail: slgu@nju.edu.cn

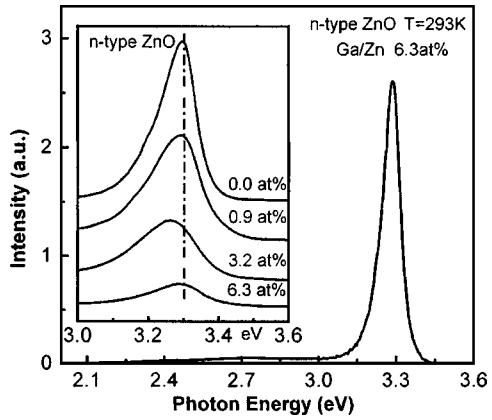

FIG. 1. Room-temperature PL spectrum of *n*-type ZnO and the inset shows the NBE transition for ZnO doped at different Ga concentration.

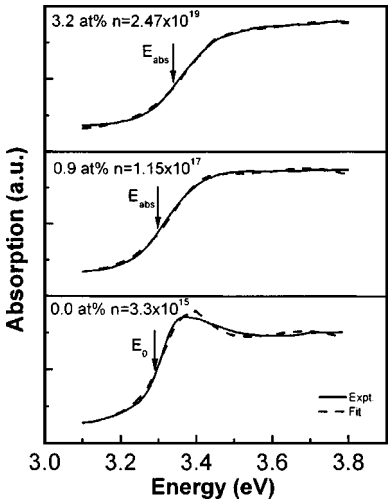

FIG. 2. The solid and dashed lines are the experimental and fitted values, respectively, of the absorption coefficient $\alpha(E)$ in the region of the direct band gap derived from transmittance spectra through the relation of $\alpha = (\log 1/T)1/d$. Indicated by arrows are the fundamental absorption edges obtained.

believed that the reduction of NBE transition energy can be interpreted as the result of the doping-induced BGR effect.[12,13] This effect is usually due to free-carrier screening and can be evaluated by an empirical relation, as reported for GaAs (Ref. 12) and GaN (Ref. 6) materials,

$$\Delta E_{\mathrm{PL}} = E_g - E_0 = -Kn^{1/3}, \tag{1}$$

where E_0 is the intrinsic energy-band gap, and E_g is the energy-band gap in the presence of excess carriers. The $n^{1/3}$ dependence of ΔE_{PL} resembles the prevailing exchange contribution of electron-electron interaction. As shown in Fig. 3(a), our experimental data are fitted well by Eq. (1). The BGR coefficients (K) evaluated by the least-squares fitting were derived to be 1.3×10^{-5} meV cm. The present K value is in good agreement with the value approximated in Ref. 8 and somewhat weaker than that in Si-doped GaN (Ref. 14) due to the difference in dielectric constant and conduction-band effective mass. Moreover, Fig. 1 shows that the peak intensities of NBE emissions decreased with increasing dopant concentration, consistent with the results for Si-doped AlN films.[14] This implies an increased nonradiative compensating native defects density with an increase of Ga doping concentration. And also, the linewidth of NBE emission broadened with increasing dopant concentration. Randomly distributed impurities unavoidably give rise to potential fluctuation or tail states of band edges, resulting in the broadening of the luminescence line, and higher compensation always leads to a greater potential fluctuation for a fixed-carrier concentration.[6] The band-gap broadening effect in highly Ga-doped ZnO films has been also observed recently by another group.[9] Apart from broadening due to deliberately doped Ga donors, the residual acceptors also contribute to the luminescence broadening.

Solid lines of Fig. 2 show the carrier concentration dependence of experimental values of the absorption coefficient, which are derived from the relation $\alpha = (\log 1/T)1/d$,[15] where T is the value of transmittance and, d is the film thickness. The data have been fitted using a comprehensive model based on the electronic energy-band structure near the optical band gap with excitonic effects. In the fundamental absorption region, the BM shift has been taken into account by the introduction of a Fermi-level filling factor (FLFF).[15] The quantity α is thus written as

$$\alpha(E) = \frac{A}{\{1+\exp[(E_{\mathrm{abs}}-E)/kT^*]\}E}\left[\frac{R_0\Gamma_0}{(E_0-R_0-E)^2+\Gamma_0^2} + \int_{E_0}^{+\infty}\frac{1}{1-\exp[-2\pi z(E')]}\frac{\Gamma_0 dE'}{(E-E')^2+\Gamma_0^2}\right], \tag{2}$$

where E is the photon energy, the term $\{1+\exp[(E_{\mathrm{abs}}-E)/kT^*]\}$, is the FLFF, E_{abs} is the absorption edge, Γ_0 is the broadening parameter for both the discrete and continuum exciton terms, $z(E)=[R_0/(E-E_0)]^{1/2}$, R_0 is the exciton binding energy (59 meV). The parameter kT^* is adjustable so as to take into account inhomogeneous broadening effect. In Eq. (2), the first and second terms in the square brackets are the contributions of the discrete and continuum excitons, respectively.[16] The dashed lines of Fig. 2 are the results of this fitting scheme, in surprisingly good agreement with the experimental data over a sufficiently wide energy region. The deduced fitting parameters are shown in Table I. For the undoped sample (S0), the FLFF was not included so that for this case $E_{\mathrm{abs}}=E_0$. The fitted results clearly demonstrated an expected blueshift of E_{abs} related to the BM effect with increasing carrier concentration.

According to parabolic-band theory,[17] the absorption edge shift ΔE_{abs} is given by

$$\Delta E_{\mathrm{abs}} = \left(\frac{\hbar^2}{2m^*}\right)(3\pi^2 n)^{2/3} - E_{\mathrm{BGR}}, \tag{3}$$

where E_{BGR} is due to the BGR effect. Using Eq. (3) with conduction and hole effective masses of 0.28 and 0.59 (in units of the free-electron mass),[18] respectively, and neglecting E_{BGR}, we have obtained solid curve in Fig. 3(b). However, this has a large disagreement with the experimental data, because this calculation is based on the assumption of a single-parabolic conduction band with a fixed value of electron effective mass (m^*). In fact, the conduction band shows a nonparabolic nature in the case of heavily doped semiconductors, and m^* increased with the increment of carrier concentration, similar with the trend in ZnO: Al films.[19] According to the Pisarkiewicz model,[20] the effective mass for a wide-band-gap semiconductor can be expressed as

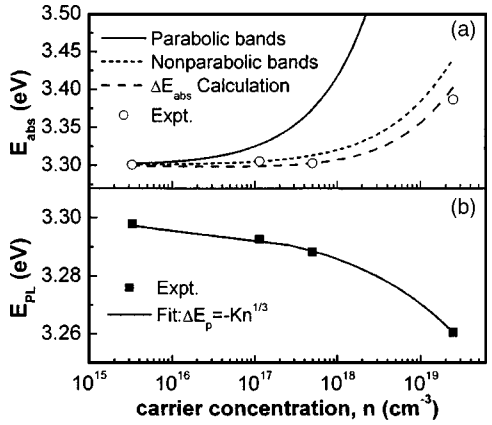

FIG. 3. The dependence of peak energy positions (a) E_{PL} and (b) E_{abs} on the carrier concentration. In (a), the solid line is the least-squares fit to data with Eq. (1). In (b), the solid and dotted lines are theoretical calculations of the BM shift according to parabolic-band and nonparabolic-band theory, respectively. The dashed line represents a calculation for ΔE_{abs} considering the nonparabolic band and BGR effects.

$$m^* = m_0^* \left[1 + 2C \frac{\hbar^2}{m_*^*} (3\pi n)^{2/3} \right]^{1/2}, \tag{4}$$

where m_0^* is the effective mass at the bottom of the conduction band. Substituting Eq. (4) into Eq. (3), we modified our calculation as shown by the dotted line in Fig. 3(b). This simulation is closer to the experimental data, indicating that the BM shift in our study exhibits nonparabolic effects. Moreover, the BGR effect has a somewhat small contribution to the BM shift. Taking account of the BGR values from PL study, we obtained the dashed line in Fig. 3(b), which provides a description for $\Delta E_{\mathrm{abs}}(n)$ as a function of the carrier concentration. The bit differences between the calculation for $\Delta E_{\mathrm{abs}}(n)$ and our experimental results are probably due to other BGR effects not considered, such as band tailing.

In summary, we have investigated the optical properties of Ga-doped ZnO epilayers grown on sapphire by MOCVD. Room-temperature PL spectra show a monotonic redshift in the near-band-gap transition energy with increasing carrier concentration. Considering the many-body theory, the BGR coefficient for ZnO is derived to be 1.3×10^{-5} meV cm. The broadening of NBE emission with increasing dopant concentration is due to the local potential fluctuations caused by randomly distributed doping impurities. The doping-induced BM effect has also been observed for the blueshift of absorption edges. The Fermi-level shift exhibits a nonparabolic nature of conduction band. The BM displacements of this work are in good agreement with the theoretical calculation based on a comprehensive model in which nonparabolic effect and BGR effects are considered.

This research was supported by special funds from the Major State Basic Research Project of China (Project No. G001CB3095), National Natural Science Foundation of China (Project Nos. 60276011 and 60390073), and Project of High Technology Research and Development of China (Project No. 2002AA311060).

[1] Y. Chen, H. Ko, S. Hong, and T. Yao, Appl. Phys. Lett. **76**, 559 (2000).
[2] W. I. Park, S. J. An, G. C. Yi, and H. M. Jiang, J. Mater. Res. **16**, 1358 (2002).
[3] T. Aoki, Y. Hatanaka, and D. C. Look, Appl. Phys. Lett. **76**, 3257 (2000).
[4] J. D. Ye, S. L. Gu, S. M. Zhu, T. Chen, L. Q. Hu, F. Qin, R. Zhang, Y. Shi, and Y. D. Zheng, J. Cryst. Growth **243**, 151 (2002).
[5] E. F. Schubert, I. D. Goepfert, W. Grieshaber, and J. M. Redwing, Appl. Phys. Lett. **71**, 921 (1997).
[6] I. Lee, J. J. Lee, P. Kung, F. J. Sanchez, and M. Razeghi, Appl. Phys. Lett. **74**, 102 (1999).
[7] K. Zhu, M. L. Nakarmi, K. H. Kim, J. Y. Lin, and H. X. Jiang, Appl. Phys. Lett. **85**, 4669 (2004).
[8] D. C. Reynolds, D. C. Look, and B. Hogai, J. Appl. Phys. **88**, 5760 (2000).
[9] T. Makoni, Y. Segawa, S. Yoshida, A. Tsukazaki, A. Ohtomo, and M. Kawasaki, Appl. Phys. Lett. **85**, 759 (2004).
[10] H. Matsui, H. Saeki, H. Tabata, and T. Kawai, J. Electrochem. Soc. **150**, G508 (2003).
[11] N. Roberts, R. P. Wang, A. W. Sleight, and W. W. Warren, Phys. Rev. B **57**, 5734 (1998).
[12] H. C. Casey, Jr. and F. Stern, J. Appl. Phys. **47**, 631 (1976).
[13] X. Zhang, S. J. Chua, W. Liu, and K. B. Chong, Appl. Phys. Lett. **72**, 1890 (1998).
[14] K. B. Nam, M. L. Nakarmi, J. Li, J. Y. Lin, and H. X. Jiang, Appl. Phys. Lett. **83**, 2787 (2003).
[15] A. R. Goni, A. Cantarero, K. Syassen, and M. Cardona, Phys. Rev. B **41**, 10111 (1990).
[16] M. Munoz, F. H. Pollak, M. Kahn, D. Ritter, L. Kronik, and G. M. Cohen, Phys. Rev. B **63**, 233302 (2001).
[17] E. J. Johnson, in *Semiconductors and Semimetals* Vol. 3, edited by R. K. Williardson and A. C. Beer (Academic, New York, 1967), p. 154.
[18] B. E. Sernelius, K. F. Berggren, Z. C. Jin, I. Hamberg, and C. G. Granqvist, Phys. Rev. B **37**, 10244 (1988).
[19] A. V. Singh, R. M. Mehra, A. Yoshiba, and A. Wakahara, J. Appl. Phys. **95**, 3640 (2004).
[20] T. Pisarkiewicz, K. Zakrzewska, and E. Leja, Thin Solid Films **174**, 271 (1989).